Heliyon 10 (2024) e31839

Contents lists available at ScienceDirect

Heliyon

journal homepage: www.cell.com/heliyon

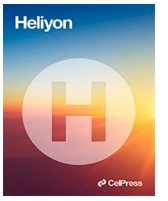

Research article

A smart detection method for sleep posture based on a flexible sleep monitoring belt and vital sign signals

Chunhua He [a], Zewen Fang [a], Shuibin Liu [a], Heng Wu [b,*], Xiaoping Li [a,**], Yangxing Wen [c,***], Juze Lin [d]

[a] School of Computer, Guangdong University of Technology, Guangzhou, 510000, PR China
[b] School of Automation, Guangdong University of Technology, Guangzhou, 510000, PR China
[c] The First Affiliated Hospital, Sun Yat-Sen University, Guangzhou, 510080, PR China
[d] Guangdong Provincial People's Hospital, Guangzhou, 510080, Guangdong, PR China

ARTICLE INFO

Keywords:
Sleep posture detection
Sleep monitoring belt
Vital signals
Feature extraction
Machine learning

ABSTRACT

People spend approximately one-third of their lives in sleep, but more and more people are suffering from sleep disorders. Sleep posture is closely related to sleep quality, so related detection is very significant. In our previous work, a smart flexible sleep monitoring belt with MEMS triaxial accelerometer and pressure sensor has been developed to detect the vital signs, snore events and sleep stages. However, the method for sleep posture detection has not been studied. Therefore, to achieve high performance, low cost and comfortable experience, this paper proposes a smart detection method for sleep posture based on a flexible sleep monitoring belt and vital sign signals measured by a MEMS Inertial Measurement Unit (IMU). Statistical analysis and wavelet packet transform are applied for the feature extraction of the vital sign signals. Then the algorithm of recursive feature elimination with cross-validation is introduced to further extract the key features. Besides, machine learning models with 10-fold cross validation process, such as decision tree, random forest, support vector machine, extreme gradient boosting and adaptive boosting, were adopted to recognize the sleep posture. 15 subjects were recruited to participate the experiment. Experimental results demonstrate that the detection accuracy of the random forest algorithm is the highest among the five machine learning models, which reaches 96.02 %. Therefore, the proposed sleep posture detection method based on the flexible sleep monitoring belt is feasible and effective.

1. Introduction

In recent years, there has been a noticeable increase of sleep disorders among individuals, leading to a decline in sleep quality and consequent feelings of restlessness and anxiety [1,2]. Sleep posture influencing sleep quality has been widely acknowledged. Specific sleeping behaviors may give rise to various health complications, such as pressure ulcers [3], restless leg syndrome and periodic leg movements [4]. Therefore, to make a correct diagnosis, it is necessary to use motion capture technique to monitor the sleep posture.

* Corresponding author.
** Corresponding author.
*** Corresponding author.
E-mail addresses: heng.wu@foxmail.com (H. Wu), xpli@gdut.edu.cn (X. Li), wenyx5@mail.sysu.edu.cn (Y. Wen).

https://doi.org/10.1016/j.heliyon.2024.e31839
Received 11 September 2023; Received in revised form 31 March 2024; Accepted 22 May 2024
Available online 30 May 2024

Considering that sleep quality has close association with sleep posture, more and more research institutes pay attention to the relevant detection techniques. Nowadays, wearable and non-wearable sleep posture detection methods have been proposed.

Polysomnography (PSG) is widely used as the gold standard for evaluating sleep quality [5,6]. It is utilized to evaluate insomnia and abnormal physical activity during sleep. Although it is the most accurate method for sleep analysis, it requires subjects to wear multiple sensors in specific positions, which makes the user intrusive and uncomfortable. Hence, there is a need to explore the non-intrusive detection methods. Seismocardiography (SCG) and Gyrocardigraphy (GCG) measure the local vibration induced by the heartbeat [7,8], and an accelerometer or a gyroscope should be worn in front of the chest [9,10]. Forcecardiography (FCG) is a new technique for measuring local vibrations caused by the heartbeat on the chest wall, and a force sensitive resistor (FSR) sensor should be mounted in front of the chest [11]. Inertial Measurement Unit (IMU), including triaxial accelerometers, and gyroscopes, can be used to detect the sleep posture, since the accelerations and angular velocities caused by heartbeat and respiration vary with the sleep posture [12]. As a result, MEMS (MicroElectroMechanical System) IMU can be embedded in wristbands or chest straps for sleep posture detection [13–15]. Although these detection techniques are effective, wearable devices may make the user uncomfortable, and they need to be charged frequently.

In addition, some non-wearable devices can be also applied for sleep posture detection. The smart mattress can be used to recognize the sleep posture with the pressure signals measured by the pressure sensors [16–20]. For illustrating the pressure map, more pressure sensors are essential, resulting in the high cost. Camera-based methods, such as optical [21,22], thermal [23] and depth cameras [24, 25], can be utilized for sleep posture detection. The detection accuracy of optical camera is very high, but it may induce privacy issues since the body of the subject is clearly visible [21,22,26–28]. The detection accuracy of thermal camera is very high since it can work under the condition of varying illumination [23] but the cost is very high. Depth camera recognizes the sleep posture based on the outline of the body, and it can protect privacy and work well even in the absence of visible light at night [24,25]. Its accuracy is high, but the cost is also high. Moreover, the installation of each camera is very complex since it should be aimed at the bed and not obstructed [22–29]. Radio frequency (RF) sensors, such as single-tone continuous Frequency Modulated Continuous Wave (FMCW), ultra-wideband (UWB), and millimeter-wave radar sensors, are also suitable for monitoring sleep posture and vital signs [30–32]. These sensors generally offer high detection accuracy but can be susceptible to interference when multiple people are present in the same area.

Ballistocardiography (BCG) measures the whole body recoil or ballistic forces generated by the heartbeat [7], and the sensor is placed between the mattress and the chest. It does not require wearing the product on the chest, so this scheme is widely popular, and some relevant studies have been reported in recent years. BCG scheme is mainly based on flexible thin-film sensors. Sensors made of flexible and thin-film materials can generate electrical signals when subjected to mechanical deformation. PolyVinyliDeneFluoride (PVDF) films and electromechanical films (EMF) [33]are commonly used materials for detecting heart rate, respiration rate and sleep movement. The products fabricated with the flexible thin-film sensors exhibit high sensitivity [34–36], thus these sensors have immense potential for health monitoring. In our previous work, a smart flexible sleep monitoring belt with MEMS triaxial accelerometer and pressure sensor has been developed to detect the vital signs, snore events and sleep stages [37]. However, the method for sleep posture detection has not been studied. Hence, to achieve high performance, low cost and comfortable experience, this paper will propose a smart detection method for sleep posture based on a flexible sleep monitoring belt and vital sign signals. In addition, in our previous work, a second-order low-pass filter has been applied to separate the heartbeat signal and respiration signal. However, this separation method is not the best, which can be replaced by Wavelet Packet Transform (WPT) algorithm.

On the other hand, sleep posture algorithm is also very important. Recently, machine learning and deep learning are widely used in sleep posture recognition. According to the reported papers, there are two main classifiers, namely image-based classifier and vital signs [38,39] based classifier. For image-based classifier, image data obtained by optical, thermal, depth or pressure sensor are fed into this classifier to identify the sleep posture. Support vector machine (SVM), ResNet, Convolutional Neural Networks (CNN), Hidden Markov Model (HMM) are adopted for feature extraction and sleep posture recognition, and the detection accuracy ranges from 83.0 % to 99.8 % [16,17,19,40,41]. The detection accuracies of some image-based classifiers are very high, especially for deep learning models, but their implementations are costly and difficult to be realized in the edge processors. For vital signs based classifier, vital sign signals acquired by MEMS IMU, ElectroCardioGraphy (ECG), BCG, SCG or GCG device are fed into this classifier to identify the sleep posture. After pre-processing of the vital sign signals, K-nearest neighbor (KNN), Naive Bayes (NB), Decision Tree (DT), ExtraTree (ET), K-means clustering, Swin Transformer (ST), SVM, CNN are adopted for feature extraction and sleep posture recognition, and the detection accuracy ranges from 80.8 % to 99.67 % [32,42–46]. The detection accuracies of some vital signs based classifiers are very high, especially for machine learning models. Therefore, in order to implement sleep posture recognition algorithms in low-cost edge processors, this work will adopt machine learning model. Meanwhile, the features of the vital sign signals are extracted and used as the inputs of the model.

Therefore, for achieving high performance, low cost, and comfortable experience, the goal of this work is to recognize the sleep posture based on the vital sign signals detected by the sleep monitoring belt. Besides, multiple machine learning algorithms, such as DT, Random Forest (RF), SVM, Extreme Gradient Boosting (XGBoost) and Adaptive Boosting (AdaBoost), will be applied for recognition and comparison. Finally, Recursive Feature Elimination with Cross-Validation (RFECV) algorithm will be introduced to screen the key features to advance the detection accuracy.

2. Materials and methods

2.1. System design

The flexible sleep monitoring belt has been developed in our previous work [37], as shown in Fig. 1. It mainly consists of a Digital Signal Processor (DSP) circuit and a flexible sensor film. The DSP circuit mainly includes the power supply subsystem, processor subsystem and sensor subsystem. The flexible Polyethylene Terephthalate (PET) film inside the belt consists of a pressure sensor array and a MEMS IMU that mounted on a Flexible Printed Circuit (FPC). The MEMS IMU (ISM330DLC, powered by STMicroelectronics NV, Paris, France) is applied to acquire the weak vibration signals, such as triaxial accelerations and angular velocities induced by heartbeat and respiration. Besides, the body movement can be also detected by the IMU. These signals vary with the sleep posture, hence the sleep posture can be recognized with the vibration signals. Additionally, the pressure sensor array is applied to detect the in-and-out-of-bed state of the user. The structure and operational principle of the pressure sensor unit are depicted in Fig. 2. The threshold of the pressure sensor unit is set as 20gf, which can filter the interferences induced by some quilts and mats. If the force exerted to the button exceeds 20gf, the pressure switch is activated (On); otherwise, it remains deactivated (off). Hence, based on the outputs of this pressure sensor array and the vital signs, it is easy to judge whether there is a person lying on the bed. Only if someone is lying on the bed will the sleep posture detection be enabled. Finally, an ARM processor (powered by STMicroelectronics NV, Paris, France) is chosen as the core Microprogrammed Control Unit (MCU) to implement the core algorithms for sleep posture detection.

Based on the smart flexible sleep monitoring belt, the experimental platform is set up, as shown in Fig. 3. The platform is composed of three parts (Data Acquisition, Data Preprocessing and Sleep Posture Classification). In the first part, the smart sleep monitoring belt is used to collect the raw signals. The flexible belt is fixed on the mattress and under the bed sheet. Since the belt is as thin as 1.5 mm, the user lying on the bed can not feel its presence. In the second part, the raw signals are preprocessed and the features of the time domain and frequency domain are extracted. In the third part, these extracted features are used as the inputs of the machine learning models for sleep posture classification.

2.2. Subject recruitment and data collection

All recruited participants received the oral and written descriptions of the experiment before starting the experiment, signed informed consent forms, and obtained approval from the institutional review committee (reference number: GDUTXS2023220). The inclusion criterion included healthy adults aged over 18. In this study, 15 young adults (5 females and 10 males) were recruited. Exclusion criterion included somebody who suffered from serious illnesses or had difficulty in maintaining or switching specific postures on the bed. During the experimental tests, the subjects lied on the bed with the flexible belt under the chest, as shown in Fig. 4. They were required to lie on the bed with four different postures, in the order of (1) supine posture, (2) right latericumbent posture, (3) left latericumbent posture, and (4) prone posture. For each posture, the relevant data were acquired for 15 min. That is, 60 min of data collection were conducted for each subject separately. Simultaneously, these data were labeled manually and saved for the further analysis.

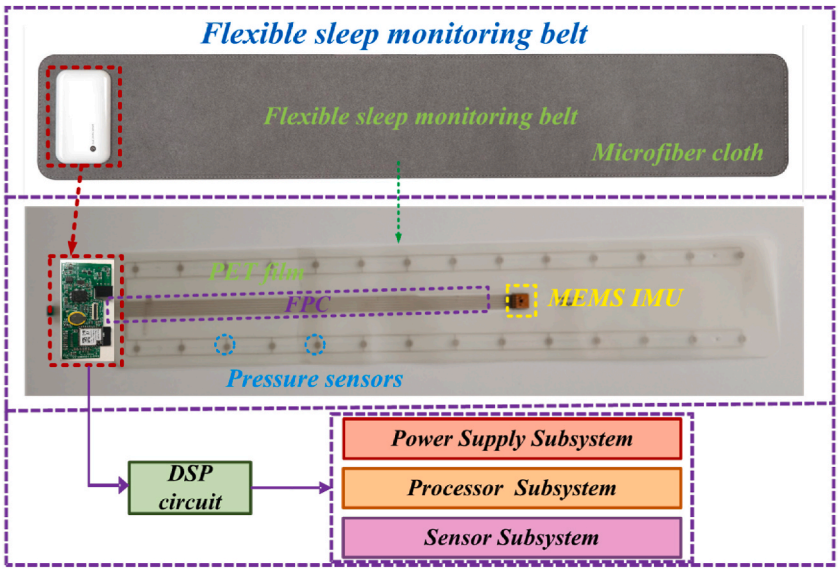

Fig. 1. Photograph of a smart flexible sleep monitoring belt.

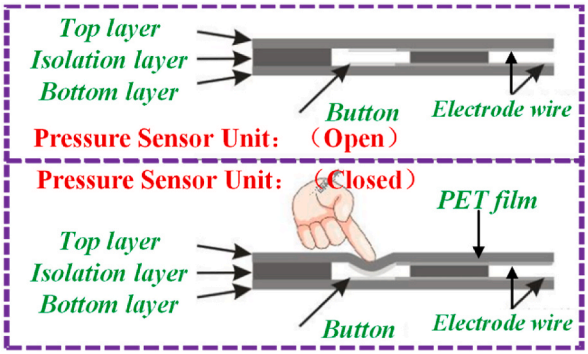

Fig. 2. Structure and operation principle of a pressure sensor unit.

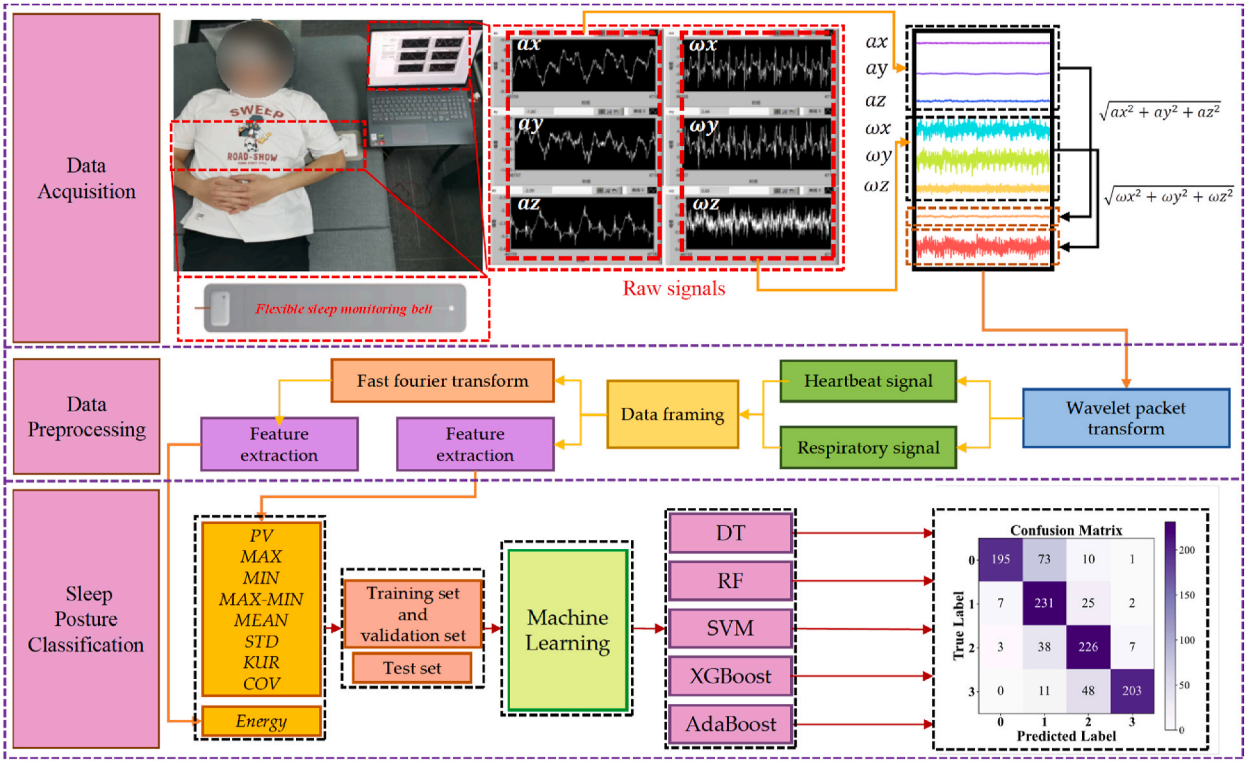

Fig. 3. Experimental platform for sleep posture recognition with the smart flexible belt.

2.3. Data Preprocessing method

Here, we take x-axis accelerometer as an example. The outputs of the x-axis accelerometer at the four sleep postures are illustrated in Fig. 5. Since the raw signals contain the information of body movement, heartbeat, respiration and measurement noise, it is difficult to accurately recognize the sleep posture based on the raw data. In order to advance the detection accuracy, heartbeat signal and respiration signal, instead of body movement signal and measurement noise, should be extracted and separated. Given that body movement may affect the sleep posture detection, hence only if there is no body movement will the sleep posture detection be enabled. The breathing frequency is generally between 0.0625–0.5Hz, and the heartbeat frequency is generally between 0.5–2.0Hz [38,39]. Considering that it is hard to accurately separated the heartbeat signal and respiration signal from the raw signal with a second-order low-pass filter, here WPT algorithm is adopted, and the structure diagram of the 10-level WPT decomposition is shown in Fig. 6.

In this paper, the sampling frequency (f_s) of the sleep monitoring belt is set to 128Hz. Thus, as shown in Fig. 6, the reconstructed signal *S0* of the node *a10* at the 10th level stands for the baseline in the frequency band of 0–0.0625Hz. Here, $0.0625 = 128/2^{(10+1)}$. The baseline describes the bias drift of the raw signal. In addition, the reconstructed signal *S1* of the node *a7* at the 7th level stands for the envelop in the frequency band of 0–0.5Hz. Here, $0.5 = 128/2^{(7+1)}$. The envelop includes the signals of the bias drift and respiration.

Fig. 4. Four main sleep postures are detected in this work.

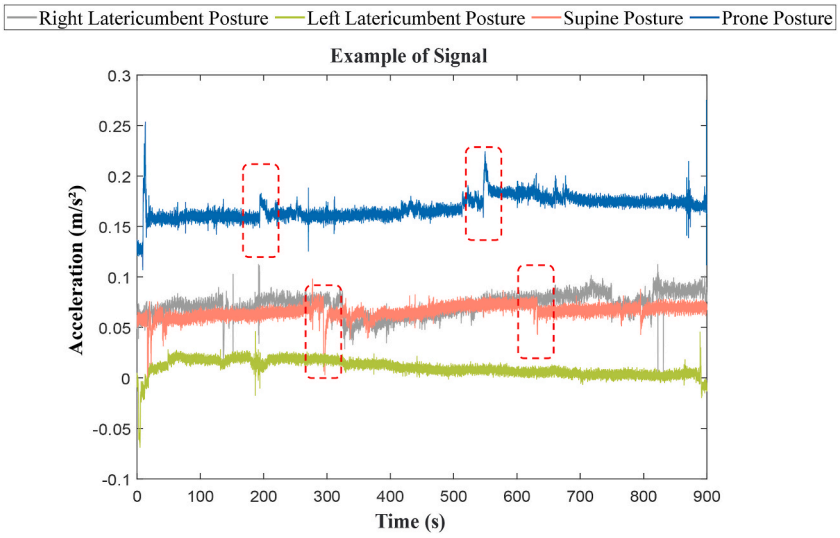

Fig. 5. Outputs of the x-axis accelerometer in the four sleep postures.

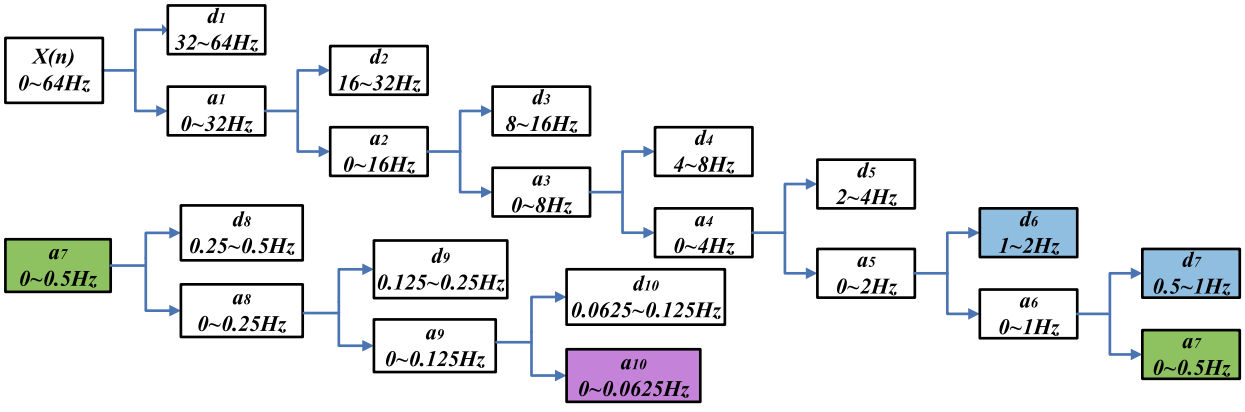

Fig. 6. Structure diagram of the 10-level WPT decomposition.

Therefore, the respiration signal can be separated, which equals to *S1* minus *S0*. Likewise, the reconstructed signal *S2* of the node *d7* represents the signal in the frequency band of 0.5 ~ 1Hz, and the reconstructed signal *S3* of the node *d6* represents the signal in the frequency band of 1 ~ 2Hz. Thus the heartbeat signal can be separated, which equals to *S2* plus *S3*. Thus, the bias drift signal (i.e.

baseline) can be separated from the raw signal, as shown in Fig. 7a. Similarly, the envelope signal, heartbeat signal and respiration signal can be separated by WPT processing, as shown in Figs. 7b–8a and 8b, respectively.

2.4. Feature extraction method

After WPT processing, the time-domain heartbeat signals of ax, ay, az, am, ωx, ωy, ωz, ωm corresponding to the four sleep postures can be obtained, as shown in Fig. 9a ax, ay, az and am represent the acceleration signals of x-axis, y-axis, z-axis and the modulus, respectively. ωx, ωy, ωz and ωm represent the angular velocity signals of x-axis, y-axis, z-axis and the modulus, respectively. In order to obtain more features, Fast Fourier Transform (FFT) processing is necessary. After FFT processing for the time-domain signals, the frequency-domain heartbeat signals of ax, ay, az, am, ωx, ωy, ωz, ωm corresponding to the four sleep postures are yielded, as depicted in Fig. 9b. Similarity, the time-domain and frequency-domain respiration signals of ax, ay, az, am, ωx, ωy, ωz, ωm corresponding to the four sleep postures can be obtained, as illustrated in Fig. 9c and d. Obviously, in Fig. 9, the signals within 100s corresponding to the four sleep postures are a little different, so the sleep posture detection can be achieved based on the subtle changes in these signals.

In general, the data in a 5s window contains at least one respiration and five heartbeat, thus during data processing, the window (i.e. framing) size is set to 5s. The time-domain heartbeat signals of ax corresponding to the four sleep postures within 5s are illustrated in Fig. 10a, while the time-domain respiration signals of ax corresponding to the four sleep postures within 5s are illustrated in Fig. 10b. Likewise, the frequency-domain heartbeat and respiration signals of ax corresponding to the four sleep postures within 5s can be obtained as Fig. 10c and d, respectively.

As shown in Fig. 10a, the amplitudes of the four heartbeat signals are different, thus the central tendencies and variabilities of the signals should be also different [47]. Therefore, features such as maximum, minimum, and mean can be calculated and applied to distinguish the postures. Besides, Fig. 10c figures out that the frequency domain characteristics of different heartbeat signals within 5s are obviously different, so the frequency domain energies of the signals can be also calculated and used as the features. Likewise, similar conclusions can be drawn regarding respiration signals, as shown in Fig. 10b and d. Hence, the main features can be defined as follows:

Assume that $\boldsymbol{x}$ is the data vector sampled within 5s, and N is the size of $\boldsymbol{x}$. $\boldsymbol{f}$ is the data vector corresponding to peak or valley value within 5s, and M is the size of $\boldsymbol{f}$. Here, the peak and valley points can be quickly identified based on second-order derivatives. PV is the variance defined as (1).

$$PV = \frac{1}{N}\sum_{j=1}^{M}\left(f(j) - \frac{1}{N}\sum_{i=1}^{N}(x(i))\right)^2 \tag{1}$$

The maximum value (MAX), minimum value (MIN), mean value ($MEAN$), standard deviation (STD), kurtosis (KUR) and covariance (COV) are defined as (2).

$$MAX = \max_{1\le i\le N}(x(i)),$$

$$MIN = \min_{1\le i\le N}(x(i)),$$

$$MEAN = \bar{x} = \frac{1}{N}\sum_{i=1}^{N}(x(i)),$$

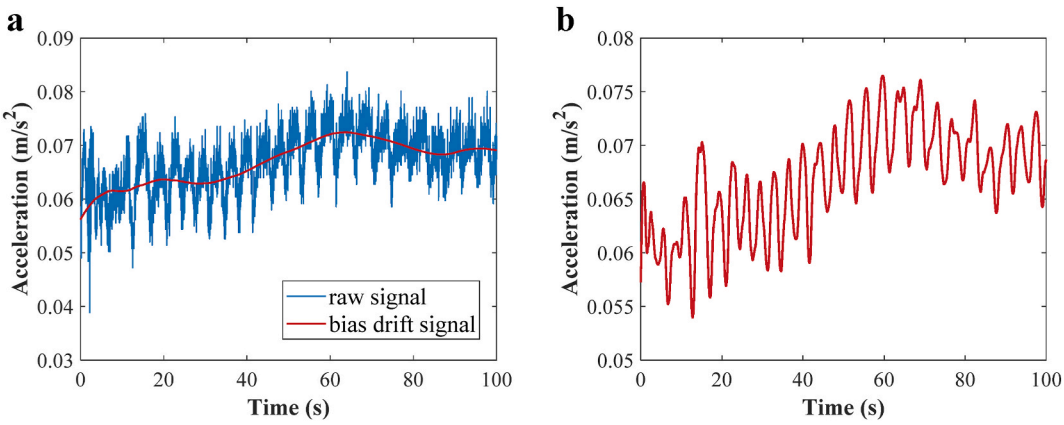

Fig. 7. (a) Raw signal and the bias drift signal; (b) Envelope signal is separated by WPT processing.

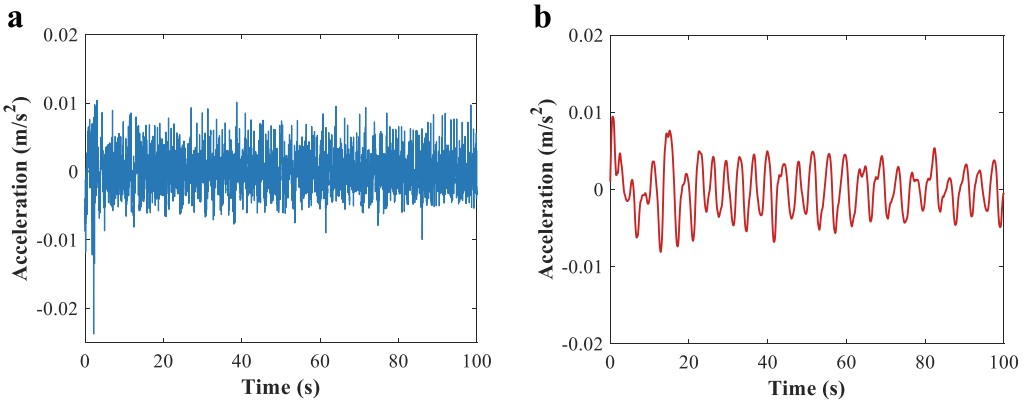

Fig. 8. (a) Heartbeat signal is separated by WPT processing; (b) Respiration signal is separated by WPT processing.

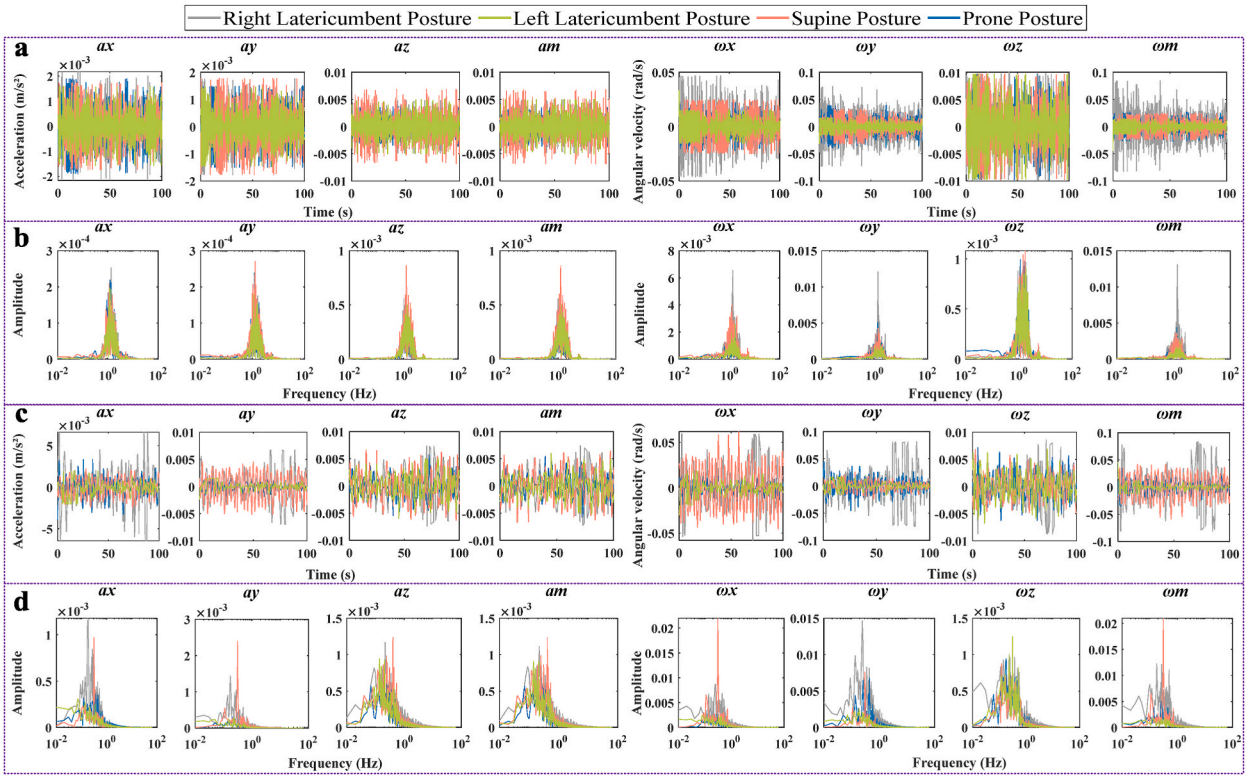

Fig. 9. (a) Time-domain heartbeat signals of ax, ay, az, am, ωx, ωy, ωz, ωm corresponding to the four sleep postures; (b) Frequency-domain heartbeat signals of ax, ay, az, am, ωx, ωy, ωz, ωm corresponding to the four sleep postures; (c) Time-domain respiration signals of ax, ay, az, am, ωx, ωy, ωz, ωm corresponding to the four sleep postures; (d) Frequency-domain respiration signals of ax, ay, az, am, ωx, ωy, ωz, ωm corresponding to the four sleep postures.

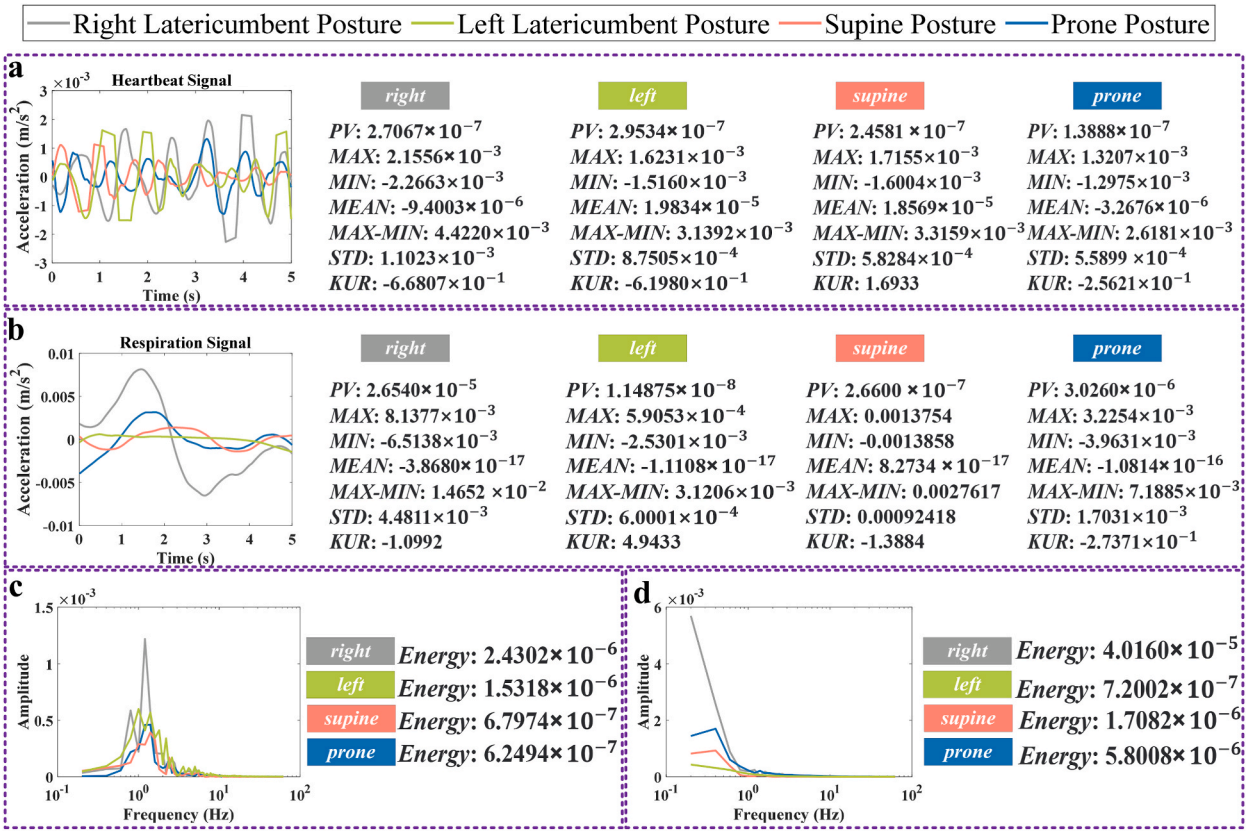

Fig. 10. (a) Time-domain heartbeat signals of *ax* corresponding to the four sleep postures within 5s; (b) Time-domain respiration signals of *ax* corresponding to the four sleep postures within 5s; (c) Frequency-domain heartbeat signals of *ax* corresponding to the four sleep postures within 5s; (d) Frequency-domain respiration signals of *ax* corresponding to the four sleep postures within 5s.

Table 1
Feature extraction with the heartbeat and respiration signals of *ax*, *ay*, *az*, *am*, *ωx*, *ωy*, *ωz* and *ωm*.

Feature	Processing object
PV	Heartbeat or respiration signals of *ax*, *ay*, *az*, *am*, *ωx*, *ωy*, *ωz*, *ωm*
MAX	Heartbeat or respiration signals of *ax*, *ay*, *az*, *am*, *ωx*, *ωy*, *ωz*, *ωm*
MIN	Heartbeat or respiration signals of *ax*, *ay*, *az*, *am*, *ωx*, *ωy*, *ωz*, *ωm*
MAX-MIN	Heartbeat or respiration signals of *ax*, *ay*, *az*, *am*, *ωx*, *ωy*, *ωz*, *ωm*
MEAN	Heartbeat or respiration signals of *ax*, *ay*, *az*, *am*, *ωx*, *ωy*, *ωz*, *ωm*
STD	Heartbeat or respiration signals of *ax*, *ay*, *az*, *am*, *ωx*, *ωy*, *ωz*, *ωm*
KUR	Heartbeat or respiration signals of *ax*, *ay*, *az*, *am*, *ωx*, *ωy*, *ωz*, *ωm*
Energy	Heartbeat or respiration signals of *ax*, *ay*, *az*, *am*, *ωx*, *ωy*, *ωz*, *ωm*
COV (*ax*, *ay*)	Heartbeat or respiration signals of *ax*, *ay*
COV (*ax*, *az*)	Heartbeat or respiration signals of *ax*, *az*
COV (*ay*, *az*)	Heartbeat or respiration signals of *ay*, *az*
COV (*ωx*, *ωy*)	Heartbeat or respiration signals of *ωx*, *ωy*
COV (*ωx*, *ωz*)	Heartbeat or respiration signals of *ωx*, *ωz*
COV (*ωy*, *ωz*)	Heartbeat or respiration signals of *ωy*, *ωz*
COV (*ax*, *ax*)	Heartbeat signal of *ax* and respiration signal of *ax*
COV (*ay*, *ay*)	Heartbeat signal of *ay* and respiration signal of *ay*
COV (*az*, *az*)	Heartbeat signal of *az* and respiration signal of *az*
COV (*ωx*, *ωx*)	Heartbeat signal of *ωx* and respiration signal of *ωx*
COV (*ωy*, *ωy*)	Heartbeat signal of *ωy* and respiration signal of *ωy*
COV (*ωz*, *ωz*)	Heartbeat signal of *ωz* and respiration signal of *ωz*

$$STD=_{\sigma}=\sqrt{\frac{1}{N}\sum_{i=1}^{N}(x(i)-\bar{x})^2}$$

$$KUR=\frac{\sum_{i=1}^{N}(x(i)-\bar{x})^4}{N\sigma^4},$$

$$COV_{xy}=\frac{1}{N-1}\sum_{i=1}^{N}(x(i)-\bar{x})(y(i)-\bar{y}),$$

$$Energy=\sum_{k=1}^{N}FX(k)^2, \tag{2}$$

Where $\boldsymbol{y}$ is another data vector sampled within 5s. $\boldsymbol{FX}$ is the data vector obtained by the FFT processing of $\boldsymbol{x}$. *Energy* is the frequency-domain energy of the framing signal. Thus, the main features can be extracted for sleep posture recognition with the heartbeat and respiration signals of ax, ay, az, am, ωx, ωy, ωz and ωm, as shown in Table 1.

2.5. Sleep posture classification method

In this paper, five machine learning algorithms, such as DT, RF, SVM, XGBoost and AdaBoost, are adopted to classify different sleep postures, their brief descriptions are as follows.

(1) DT algorithm is capable of efficiently dividing the data in a short time, making it suitable for multiclassification problems. In the DT model, the leaf nodes represent the final decision results.
(2) RF algorithm is a classifier that utilizes multiple decision trees to train and predict samples. It takes advantage of the collective prediction of multiple decision trees to enhance prediction accuracy.
(3) SVM algorithm maps the data to a multidimensional space using a kernel function, enabling the identification of a hyperplane that better separates the samples. The data's geometric properties are used to improve the performance.
(4) XGBoost algorithm is commonly used for regression and classification tasks. It builds upon the gradient-enhanced DT algorithm and combines different decision trees to make predictions, effectively boosting its predictive power.
(5) AdaBoost algorithm is an ensemble machine learning method that combines weak learners to form a strong learner. During training, it adaptively adjusts the weak learners by maintaining a collection of weights.

For machine learning, the total sample size is 10800. The sizes of the training set, validation set and test set are 8836, 982 and 982, respectively. The training set and verification set are used for 10-fold cross-validation, and the data size is 9818. The test set is used to validate the accuracy of the model after cross validation.

The hyperparameters for these machine learning models are optimized and listed in Table 2. Where, *N_estimators* is the number of decision trees in the forest, *Max_depth* is the maximum number of levels in each decision tree, *C* is the penalty factor, and *Learning_rate* is the learning rate. The selection of appropriate hyperparameters is crucial in achieving accurate and reliable classification.

2.6. Recursive feature elimination with cross-validation

RFECV algorithm is a wrapper feature selection method that uses a machine learning algorithm to screen the most key features for sleep posture detection. To ensure its robustness, it combines recursive feature elimination and cross-validation to determine the optimal number of features to maximize model performance [48]. It uses a classification machine learning model to score each feature and iteratively eliminate features that cannot improve classification accuracy. This algorithm starts with a complete feature set and gradually removes the features that do not contribute to classification accuracy, ultimately identifying the most effective feature subset. Owing to the merits, in this work, RFECV algorithm is introduced to screen the main features. The implementation of RFECV algorithm uses a random forest classification model as an estimator, with cross-validation multiple equals to 10, and *StratifiedKFold* as

Table 2
Hyperparameters are optimized for different models.

Model	Hyperparameter	Search Space	Search Interval
DT	*Max_depth*	1–30	1
RF	*N_estimators*	1–60	1
SVM	*C*	0.1–3.5	0.2
XGBoost	*N_estimators, Max_depth*	N_estimators: 2 - 80 Max_depth: 1 - 30	N_estimators: 2 Max_depth: 1
AdaBoost	*N_estimators, Learning_rate*	N_estimators: 2 -100 Learning_rate: 0.02–0.5	N_estimators: 2 Learning_rate: 0.02

the splitting strategy.

2.7. Evaluation indexes

In order to evaluate the performances of these detection methods, evaluation indexes, such as precision (*PR*), recall (*RE*), F1-Score (F_1-*Score*), and detection accuracy (*ACC*), are adopted and defined as (3).

$$PR = \frac{TP}{TP + FP},$$

$$RE = \frac{TP}{TP + FN},$$

$$F_1 - Score = \frac{2 \times RE \times PR}{RE + PR},$$

$$ACC = \frac{TP + TN}{TP + TN + FP + FN}, \tag{3}$$

Where *TP* stands for the number of true positives, *FP* stands for the number of false positives, *TN* stands for the number of true negatives, and *FN* stands for the number of false negatives. Therefore, these four parameters are the most important performance indexes.

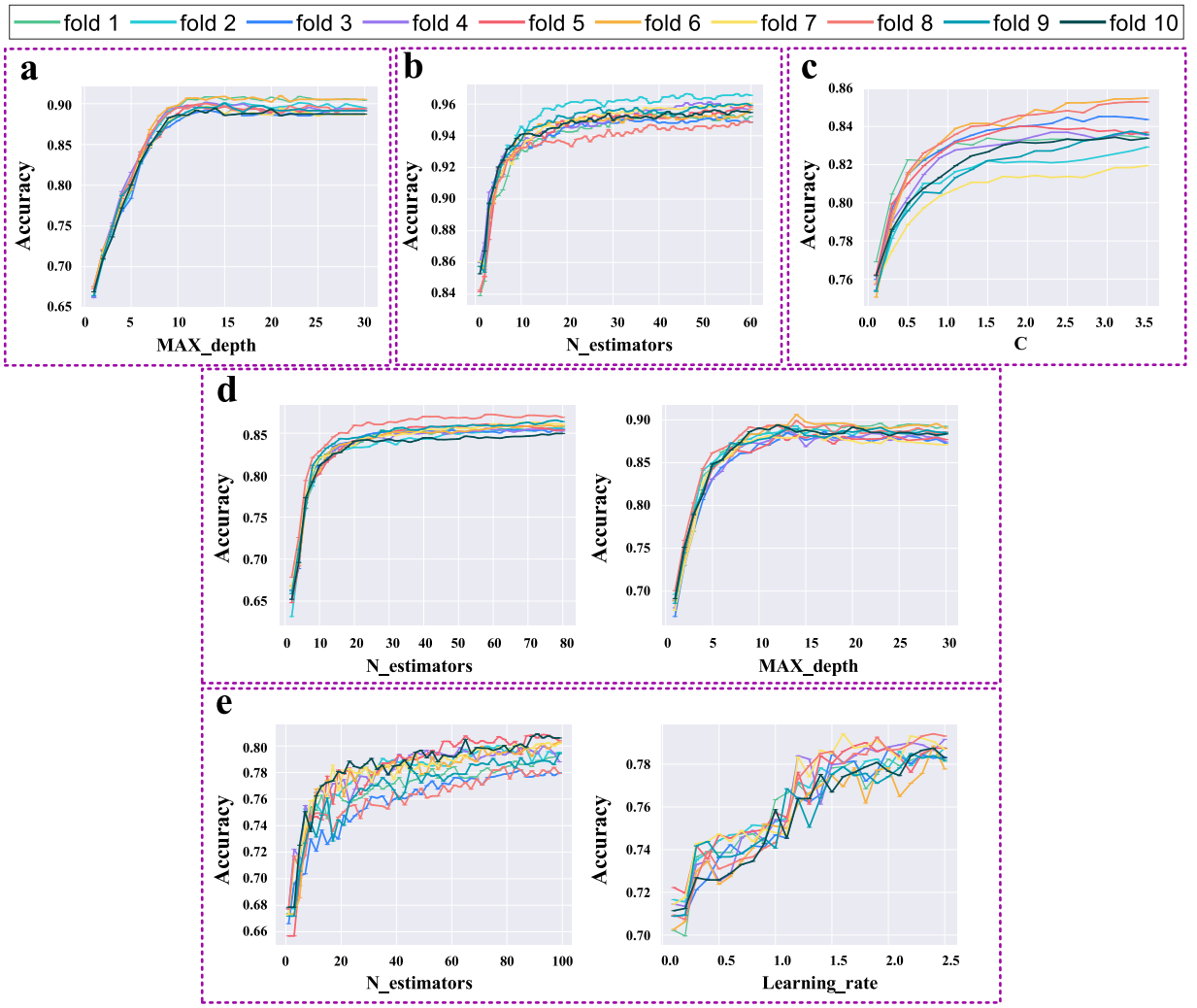

Fig. 11. Accuracy curves of different machine learning models with different hyperparameters: (a) DT; (b) RF; (c) SVM; (d) XGBoost; (e) AdaBoost.

3. Results

3.1. Hyperparameter tuning result

After hyperparameter tuning using 10-fold cross-validation, the accuracy curves of different machine learning models with different hyperparameters are illustrated in Fig. 11a-e. Based on these curves, the optimal values of the hyperparameters can be confirmed. The hyperparameter is determined when the corresponding accuracy reaches maximum. According to this principle and Fig. 11, *Max_depth* of the DT model is set to 15. *N_estimators* of the RF model is set to 50. *C* of the SVM model is set to 3. *N_estimators* and *Max_depth* of the XGBoost model are set to 50 and 15, respectively. *N_estimators* and *Learning_rate* of the AdaBoost model are set to 80 and 0.4, respectively (see Fig. 12).

3.2. Classification result before RFECV processing

The confusion matrices of the classification results of the five algorithms on the test set are shown in Fig. 12a-e, the labels 0, 1, 2, and 3 represent four sleep postures: supine posture, right latericumbent posture, left latericumbent posture, and prone posture, respectively. Elements of the confusion matrices for evaluating the five models' performances are listed in Table 3. Evaluation indexes of the five classification models are listed in Table 4. It indicates that RF model stands out with the highest performance, exhibiting accuracy, recall rate, and F1-score all exceeding 90 %. Specifically, RF model achieves an accuracy of 95.65 %. Following closely behind, DT model also performs commendably, with an accuracy of 91.44 %. As for the remaining three models, they all exhibit accuracies exceeding 80 %. In order to further advance the performance indexes, RFECV processing are adopted.

3.3. Classification result after RFECV processing

The RFECV experiment consists of two stages. In the first stage, RFECV combined with the RF model is trained and tested using all original 146 features. The goal is to determine the optimal feature set for the four-classification task of sleep posture detection. In the second stage, the features selected from the first stage are used to train and test the above five machine learning classifiers.

Fig. 13a shows the ranking of the most important 40 features. It figures out that among the top ranked features, heartbeat-related features, instead of the respiration-related features, account for the majority. Fig. 13b illustrates the relationship between classification score and the number of selected features using RFECV processing. It indicates that the number of features achieving the highest classification score is 40. Therefore, the number of original features can be reduced from 146 to 40, which makes the model simpler and easier to be realized.

Table 5 illustrates the evaluation indexes of the five classification models after RFECV processing. The comparison of the accuracies of the five classification models without and with RFECV processing is shown in Fig. 14. It shows that except for AdaBoost, other models achieve better performance with RFECV processing. It means that these screened 40 features can represent the most important information required for high-accurate classification, and data dimensionality can be effectively reduced without sacrificing the detection accuracy. After RFECV processing, the accuracy of the RF model is still the highest, which is improved to 96.02 %. By comparison, the RF model, rather than other models, is the best choice for sleep posture detection.

4. Discussion

4.1. Performance comparison

The performance comparison between the proposed method and the related work has been summarized in Table 6. It figures out that most of the related works focus on the automatic detection of the four sleep postures (i.e. supine pose, right latericubent pose, left latericubent pose, and prone pose), because the detection results have more practical value. Hence, this work also focuses on these four sleep postures detection, and in the future, more sleep postures detection will be conducted. The majority of the related studies have a sample size of over ten people, so the sample size of this work is set to 15. In terms of hardware, the cost of this work is lower than most of those of the related studies. Moreover, the flexible sleep monitoring belt is a non-wearable electronic product, which is portable, non-invasive and has no privacy issue. In terms of installation method, the installation of this work is simpler compared to the other work. In terms of detection accuracy, although the accuracies of the wearable electronic products are a litter higher than that of this work, it may make the users uncomfortable, and most users are unwilling to wear any electronic devices while sleeping.

4.2. Limitations and future work

The number of the subjects in this experiment is relatively small, mainly young people, with a slight gender imbalance, which may affect the generalization ability of the model. Specifically, the sleep habits of the elderly may be different from those of the young, and the sleep habits of men may be different from those of women, all of which challenge the performance of the model in this work. Therefore, in the future, we will recruit more subjects of different age, and keep the gender balance to ensure the external effectiveness. On the other hand, supine posture, right latericubent posture, left latericubent posture and prone posture are the four most common postures that provide a good basis for diagnosing sleep disorders. At present, the detection accuracy of these four sleep postures is very high. However, detection for four sleep postures is not enough. In the future, we will try to detect more sleep postures.

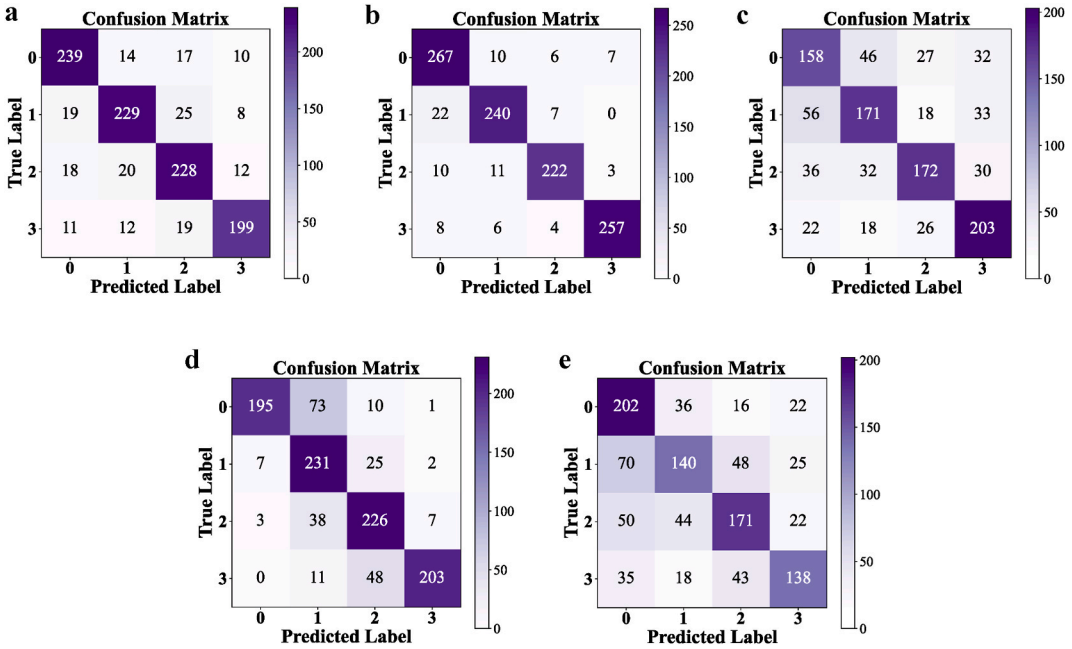

Fig. 12. Classification results of different algorithms, with 0, 1, 2, and 3 in the confusion matrix representing supine posture, right latericumbent posture, left latericumbent posture, and prone posture, respectively. (a) DT; (b) RF; (c) SVM; (d) XGBoost; (e) AdaBoost.

Table 3
Elements of the confusion matrices for evaluating the five models' performances.

Model	TP	TN	FP	FN
DT	223.75	763.75	46.25	46.25
RF	246.50	786.50	23.50	23.50
SVM	176.0	716.0	94.00	94.00
XGBoost	213.75	753.75	56.25	56.25
AdaBoost	162.75	162.75	107.25	107.25

Table 4
Evaluation indexes of the five classification models before RFECV processing.

Model	Precision	Recall	F1-Score	Accuracy
DT	83.09 %	82.86 %	82.95 %	91.44 %
RF	91.50 %	91.25 %	91.35 %	95.65 %
SVM	65.26 %	65.19 %	65.12 %	82.59 %
XGBoost	82.25 %	79.26 %	79.58 %	89.58 %
AdaBoost	60.90 %	60.30 %	60.17 %	80.14 %

5. Conclusion

In this paper, a smart detection method for sleep posture based on a flexible sleep monitoring belt is proposed. The feature extraction method and five machine learning models have been described in detail. RFECV algorithm is introduced to further extract the key features. Experimental results demonstrate that the detection accuracy of the random forest algorithm is the highest among the five machine learning models, which reaches 96.02 %. Therefore, the proposed sleep posture detection method based on the flexible sleep monitoring belt is feasible and effective. In the future, more subjects of different age will be recruited and tested to further validate the effectiveness of the proposed detection method.

Data availability statement

The authors do not have permission to share data.

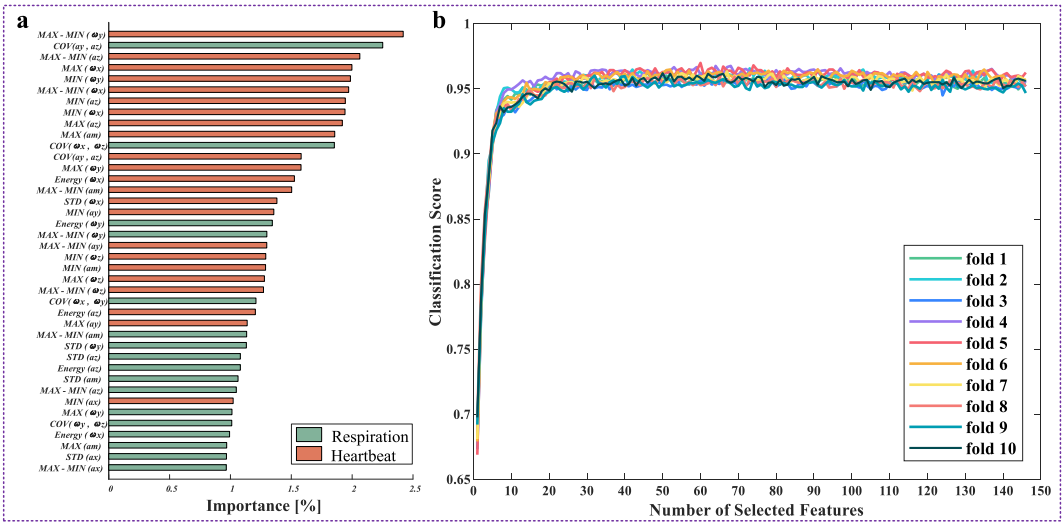

Fig. 13. (a) Ranking of the most important 40 features; (b) Relationship between classification score and the number of selected features using RFECV processing.

Table 5
Evaluation indexes of the five classification models after RFECV processing.

Model	Precision	Recall	F1-Score	Accuracy
DT	83.27 %	83.15 %	83.17 %	91.57 %
RF	92.12 %	92.06 %	92.07 %	96.02 %
SVM	67.02 %	67.04 %	66.99 %	83.56 %
XGBoost	83.66 %	81.47 %	81.57 %	90.65 %
AdaBoost	59.39 %	58.84 %	58.75 %	79.44 %

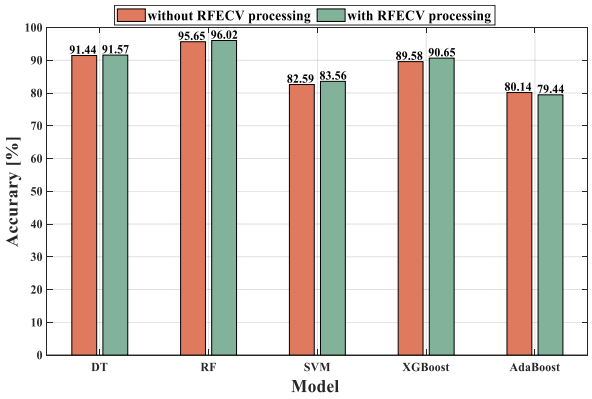

Fig. 14. Comparison of the accuracies of the five classification models without and with RFECV processing.

Ethics declarations

This study was reviewed and approved by the ethics committee of Guangdong University of Technology, with the approval number: GDUTXS2023220.

CRediT authorship contribution statement

Chunhua He: Writing – review & editing, Funding acquisition, Conceptualization. **Zewen Fang:** Writing – original draft, Software, Investigation. **Shuibin Liu:** Visualization, Software. **Heng Wu:** Validation, Project administration, Methodology. **Xiaoping Li:** Writing – review & editing, Data curation. **Yangxing Wen:** Resources, Data curation. **Juze Lin:** Writing – review & editing, Formal analysis.

Table 6
Performance comparison between the proposed method and the related work.

Source	Hardware	Installation method	Classifier	Sample size	The number of sleep postures	Accuracy
[40]	A thermopile array sensor	On the ceiling and bedside	SVM	12	9	99.80 %
[41]	A 2D IR camera	Above the bed	ResNet-152	12	4	95.10 %
[16]	A pressure sensor mat	On the ground	CNN	–	5	90.00 %
[19]	A bedsheet with sensor array	On the bed	CNN	5	6	84.80 %
[17]	A dense pressure sensitive bed sheet system	On the bed	HMM	14	6	83.00 %
[42]	Three wearable accelerometer sensors	Two on each arm and one on the chest	KNN, NB and DT	10	4	99.50 %
[43]	A single wearable device	On the neck	ExtraTrees classifier	18	4	99.00 %
[44]	A fabric-sheet unified sensing electrode	On the bed	K-means clustering	7	2	88.00 %
[32]	Three IR-UWB radar sensors	On the ceiling and bedside	Swin Transformer	30	4	80.80 %
[46]	An impedance instrument, multi-channel adapter	On the subject's body	SVM	16	4	99.67 %
[27]	An IR camera	Above the bed	CNN	12	12	91.00 %
This work	A flexible sleep monitoring belt	On the mattress and under the bed sheet	RF	15	4	96.02 %

Declaration of competing interest

The authors declare that they have no known competing financial interests or personal relationships that could have appeared to influence the work reported in this paper.

Acknowledgements

This work was supported by the National Natural Science Foundation of China (Grant Nos. 62104047, U22A2012 and 62173098), Guangdong Basic and Applied Basic Research Foundation (Grant No. 2023A1515010291), and Basic and Applied Basic Research Foundation of Guangzhou Basic Research Program (Grant No. 2023A04J1707).

References

[1] D.J. Buysse, R. Grunstein, J. Horne, P. Lavie, Can an improvement in sleep positively impact on health? Sleep Med. Rev. 14 (2010) 405–410.
[2] T.L. Sletten, et al., The importance of sleep regularity: a consensus statement of the National Sleep Foundation sleep timing and variability panel, Sleep Health 9 (2023) 801–820.
[3] L. Paquay, R. Wouters, T. Defloor, F. Buntinx, R. Debaillie, L. Geys, Adherence to pressure ulcer prevention guidelines in home care: a survey of current practice, J. Clin. Nurs. 17 (2008) 627–636.
[4] V. Ibanez, J. Silva, O. Cauli, A survey on sleep assessment methods, PeerJ 6 (2018) e4849.
[5] J. Wang, S. Zhao, Y. Zhou, H. Jiang, Z. Yu, T. Li, S. Li, G. Pan, Narcolepsy diagnosis with sleep stage features using PSG recordings, IEEE Trans. Neural Syst. Rehabil. Eng. 31 (2023) 3619–3629.
[6] B.V. Vaughn, P. Giallanza, Technical review of polysomnography, Chest 134 (2008) 1310–1319.
[7] X. Han, et al., The latest progress and development trend in the research of ballistocardiography (BCG) and seismocardiogram (SCG) in the field of health care, Appl. Sci. 11 (2021) 8896.
[8] Y. D' Mello, et al., Real-time cardiac beat detection and heart rate monitoring from combined seismocardiography and gyrocardiography, Sensors 19 (2019) 3472.
[9] M.J. Tadi, et al., Gyrocardiography: a new non-invasive monitoring method for the assessment of cardiac mechanics and the estimation of hemodynamic variables, Sci. Rep. 7 (2017) 6823.
[10] S. Morra, et al., Ballistocardiography and seismocardiography detection of hemodynamic changes during simulated obstructive apnea, Physiol. Meas. 41 (2020) 065007.
[11] E. Andreozzi, A. Fratini, D. Esposito, G. Naik, C. Polley, G.D. Gargiulo, P. Bifulco, Forcecardiography: a novel technique to measure heart mechanical vibrations onto the chest wall, Sensors 20 (2020) 3885.
[12] C. Massaroni, C. Romano, F. De Tommasi, M.B. Cukic, M. Carassiti, D. Formica, E. Schena, Heart rate and heart rate variability indexes estimated by mechanical signals from A skin-interfaced IMU, in: 2022 IEEE International Workshop on Metrology for Industry 4.0 & IoT (MetroInd4. 0&IoT), IEEE, 2022, pp. 322–327.
[13] L. Chang, J. Lu, J. Wang, X. Chen, D. Fang, Z. Tang, P. Nurmi, Z. Wang, SleepGuard: capturing rich sleep information using smartwatch sensing data, Proceedings of the ACM on Interactive, Mobile, Wearable and Ubiquitous Technologies 2 (2018) 1–34.
[14] O.S. Eyobu, Y.W. Kim, D. Cha, D.S. Han, A real-time sleeping position recognition system using IMU sensor motion data, in: 2018 IEEE International Conference on Consumer Electronics (ICCE), IEEE, 2018, pp. 1–2.
[15] H.D. Vu, D.N. Tran, K.L. Can, T.H. Dao, D.D. Pham, D.T. Tran, Enhancing sleep postures classification by incorporating acceleration sensor and LSTM model, in: 2023 IEEE Statistical Signal Processing Workshop (SSP), IEEE, 2023, pp. 661–665.
[16] K. Tang, A. Kumar, M. Nadeem, I. Maaz, CNN-based smart sleep posture recognition system, IoT 2 (2021) 119–139.
[17] J.J. Liu, W. Xu, M.C. Huang, N. Alshurafa, M. Sarrafzadeh, N. Raut, B. Yadegar, Sleep posture analysis using a dense pressure sensitive bedsheet, Pervasive Mob. Comput. 10 (2014) 34–50.
[18] L.J. Kau, M.Y. Wang, H. Zhou, Pressure-sensor-based sleep status and quality evaluation system, IEEE Sensor. J. 9 (2023) 9739–9754.
[19] Q. Hu, X. Tang, W. Tang, A real-time patient-specific sleeping posture recognition system using pressure sensitive conductive sheet and transfer learning, IEEE Sensor. J. 21 (2020) 6869–6879.
[20] Y. Chao, T. Liu, L.M. Shen, Method of recognizing sleep postures based on air pressure sensor and convolutional neural network: for an air spring mattress, Eng. Appl. Artif. Intell. 121 (2023) 106009.
[21] L. Nuksawn, E. Nantajeewarawat, S. Thiemjarus, Real-time sensor-and camera-based logging of sleep postures, in: 2015 International Computer Science and Engineering Conference (ICSEC), IEEE, 2015, pp. 1–6.
[22] W. Huang, A.A.P. Wai, S.F. Foo, J. Biswas, C.C. Hsia, K. Liou, Multimodal sleeping posture classification, in: 2010 20th International Conference on Pattern Recognition, IEEE, 2010, pp. 4336–4339.
[23] P. Jakkaew, T. Onoye, Non-contact respiration monitoring and body movements detection for sleep using thermal imaging, Sensors 20 (2020) 6307.
[24] T. Grimm, M. Martinez, A. Benz, R. Stiefelhagen, Sleep position classification from a depth camera using bed aligned maps, in: 2016 23rd International Conference on Pattern Recognition (ICPR), IEEE, 2016, pp. 319–324.
[25] A. Ren, B. Dong, X. Lv, T. Zhu, F. Hu, X. Yang, A non-contact sleep posture sensing strategy considering three dimensional human body models, in: 2016 2nd IEEE International Conference on Computer and Communications (ICCC), IEEE, 2016, pp. 414–417.
[26] F. Deng, J. Dong, X. Wang, Y. Fang, Y. Liu, Z. Yu, J. Liu, F. Chen, Design and implementation of a noncontact sleep monitoring system using infrared cameras and motion sensor, IEEE Trans. Instrum. Meas. 67 (2018) 1555–1563.
[27] S.M. Mohammadi, M. Alnowami, S. Khan, D.J. Dijk, A. Hilton, K. Wells, Sleep posture classification using a convolutional neural network, in: 2018 40th Annual International Conference of the IEEE Engineering in Medicine and Biology Society (EMBC), IEEE, 2018, pp. 1–4.
[28] Y.K. Wang, H.Y. Chen, J.R. Chen, Unobtrusive sleep monitoring using movement activity by video analysis, Electronics 8 (2019) 812.
[29] M.S. Rasouli D, S. Payandeh, A novel depth image analysis for sleep posture estimation, J. Ambient Intell. Hum. Comput. 10 (2019) 1999–2014.
[30] S. Yue, Y. Yang, H. Wang, H. Rahul, D. Katabi, BodyCompass: monitoring sleep posture with wireless signals, Proceedings of the ACM on Interactive, Mobile, Wearable and Ubiquitous Technologies 4 (2020) 1–25.
[31] Z. Yang, P.H. Pathak, Y. Zeng, X. Liran, P. Mohapatra, Vital sign and sleep monitoring using millimeter wave, ACM Trans. Sens. Netw. 13 (2017) 1–32.
[32] D.K.H. Lai, Z.H. Yu, T.Y.N. Leung, et al., Vision transformers (ViT) for blanket-penetrating sleep posture recognition using a triple ultra-wideband (UWB) radar system, Sensors 23 (2023) 2475.
[33] S. Rajala, J. Lekkala, Film-type sensor materials PVDF and EMFi in measurement of cardiorespiratory signals-A review, IEEE Sensor. J. 12 (2010) 439–446.
[34] G. Matar, G. Kaddoum, J. Carrier, J.M. Lina, Kalman filtering for posture-adaptive in-bed breathing rate monitoring using bed-sheet pressure sensors, IEEE Sensor. J. 21 (2020) 14339–14351.
[35] L. Peng, A. Yin, W. Song, W. Yao, H. Ren, L. Yang, Sleep monitoring with hidden Markov model for physical conditions tracking, IEEE Sensor. J. 21 (2020) 14232–14239.
[36] Y. Zhang, A. Xiao, T. Zheng, H. Xiao, R. Huang, The relationship between sleeping position and sleep quality: a flexible sensor-based study, Sensors 22 (2022) 6220.

[37] C. He, J. Tan, X. Jian, G. Zhong, L. Cheng, J. Lin, A smart flexible vital signs and sleep monitoring belt based on MEMS triaxial accelerometer and pressure sensor, IEEE Internet Things J. 9 (2022) 14126–14136.
[38] G. Lorenzi-Filho, H.R. Dajani, R.S. Leung, J.S. Floras, T.D. Bradley, Entrainment of blood pressure and heart rate oscillations by periodic breathing, Am. J. Respir. Crit. Care Med. 159 (1999) 1147–1154.
[39] M.A. García-González, A. Argelagós-Palau, M. Fernández-Chimeno, J. Ramos-Castro, A comparison of heartbeat detectors for the seismocardiogram, Computing in Cardiology 2013, IEEE (2013) 461–464.
[40] Z. Chen, Y. Wang, Remote recognition of in-bed postures using a thermopile array sensor with machine learning, IEEE Sensor. J. 21 (2021) 10428–10436.
[41] S.M. Mohammadi, S. Enshaeifar, A. Hilton, D.J. Dijk, K. Wells, Transfer learning for clinical sleep pose detection using a single 2D IR camera, IEEE Trans. Neural Syst. Rehabil. Eng. 29 (2020) 290–299.
[42] R.M. Kwasnicki, G.W. Cross, L. Geoghegan, Z. Zhang, P. Reilly, A. Darzi, G.Z. Yang, R. Emery, A lightweight sensing platform for monitoring sleep quality and posture: a simulated validation study, Eur. J. Med. Res. 23 (2018) 1–9.
[43] R.S. Abdulsadig, S. Singh, Z. Patel, E. Rodriguez-Villegas, Sleep posture detection using an accelerometer placed on the neck, in: 2022 44th Annual International Conference of the IEEE Engineering in Medicine & Biology Society (EMBC), IEEE, 2022, pp. 2430–2433.
[44] M. Takano, A. Ueno, Noncontact in-bed measurements of physiological and behavioral signals using an integrated fabric-sheet sensing scheme, IEEE journal of biomedical and health informatics 23 (2018) 618–630.
[45] K. Kido, T. Tamura, N. Ono, M. Altaf-Ul-Amin, M. Sekine, S. Kanaya, M. Huang, A novel CNN-based framework for classification of signal quality and sleep position from a capacitive ECG measurement, Sensors 19 (2019) 1731.
[46] G. Liu, K. Li, L. Zheng, W.H. Chen, G. Zhou, Q. Jiang, A respiration-derived posture method based on dual-channel respiration impedance signals, IEEE Access 5 (2017) 17514–17524.
[47] N. Pradhan, S. Rajan, A. Adler, C. Redpath, Classification of the quality of wristband-based photoplethysmography signals, in: 2017 IEEE International Symposium on Medical Measurements and Applications (MeMeA), IEEE, 2017, pp. 269–274.
[48] X.W. Chen, J.C. Jeong, Enhanced recursive feature elimination, in: Sixth International Conference on Machine Learning and Applications (ICMLA 2007), IEEE, 2007, pp. 429–435.